The Journal of Experimental Biology 210, 3897-3909
Published by The Company of Biologists 2007
doi:10.1242/jeb.006940

Morphology and kinematics of feeding in hagfish: possible functional advantages of jaws

Andrew J. Clark* and Adam P. Summers

Evolutionary and Comparative Physiology, Department of Ecology and Evolutionary Biology, 321 Steinhaus Hall, University of California, Irvine, CA 92697-2525, USA

*Author for correspondence (e-mail: aclark@uci.edu)

Accepted 29 August 2007

Summary

As in gnathostomes, the hagfish feeding apparatus includes skeletal, dental and muscular components. In the present study, we examined feeding morphology and kinematics in two hagfish species, *Eptatretus stoutii* and *Myxine glutinosa*, representing the two major hagfish lineages. *E. stoutii* have larger dental plates, larger basal plates, and stronger clavatus muscles (the major dental plate retractor) than *M. glutinosa*. Despite morphological differences, kinematic profiles are similar in *E. stoutii* and *M. glutinosa*. When protracted, the dental plate unfolds and exposes keratinous teeth, which are then embedded in the prey. Once food is grasped, the dental plate is retracted into the mouth. During retraction, the clavatus muscle can generate up to 16 N of force, which exceeds the bite force of some gnathostomes of similar size. In addition to producing high forces with the feeding muscles, hagfish can evert their dental plates to 180°, exceeding the gape angles attained by virtually all gnathostomes, suggesting vertebrate jaws are not the prerequisites for muscle force generation and wide gapes. We propose that dental plate protraction and retraction can be modeled as a fixed pulley that lacks the speed amplification occurring in gnathostome jaws. Hagfish gape cycle times are approximately 1 s, and are longer than those of gnathostomes, suggesting that a functional advantage of jaws is the speed that allows gnathostomes to exploit elusive prey.

Supplementary material available online at
http://jeb.biologists.org/cgi/content/full/210/22/3897/DC1

Key words: gape cycle time, agnathan, jawless feeding, aquatic feeding, *Myxine glutinosa*, *Eptatretus stoutii*.

Introduction

From the Lower Silurian to the Upper Devonian, approximately 80 million years, a diversity of agnathans (jawless fishes) coexisted with the earliest gnathostomes (jawed vertebrates) (Carroll, 1988). Agnathans have been reduced to two successful groups, the hagfishes and lampreys, which have persisted since the Paleozoic and collectively comprise just 0.2% of extant craniates. Despite their minimal current diversity, agnathans were the most abundant craniates for over 140 million years (Purnell, 2002). Fossil agnathans were diverse, and often possessed a protective dermal layer of bone and dentine. Jawed craniates became the dominant form following the extinction of most agnathans in the late Devonian. The selective pressures on craniates in the late Devonian are not known and how jaws were initially used is unclear (Mallatt, 1996). Virtually all extant craniates have jaws that are used for various behaviors including breathing, communication, and combat. Jaws are especially important for prey capture and feeding and allow gnathostomes to exploit a variety of food types.

Hagfish are basal craniates and the sister taxon to the vertebrates (Liem et al., 2001). Unlike the lampreys, hagfish lack any traces of vertebrae and are exclusively marine (Liem et al., 2001; Martini, 1998). There are approximately 60 identified species, which are primarily recognized as demersal scavengers feeding on dead or dying marine invertebrates and vertebrates (Fernholm, 1998; Martini, 1998). Though hagfish morphology is unusual, it is highly conserved through time. The earliest known hagfish specimen (*Myxinikela siroka*), from the late Paleozoic of Illinois (approximately 300 million years ago), is morphologically similar to extant genera (Bardack, 1991). Although the phylogeny of extant hagfish is not well resolved, two subfamilies are recognized: the Myxininae and Eptatretinae (Fernholm, 1998).

The jawless feeding apparatus of hagfish is complex and functions in a very different fashion than vertebrate jaws, though it does have the same basic components: a supporting skeleton, muscles to power movement, and a dental battery to capture and process prey. Hagfish capture and transport food with two rows of non-serrated, grasping keratinous ‘teeth’, which are anchored to dental plates, a bilaterally folding, paired series of cartilages (Fig. 1A) (Cole, 1905; Cole, 1907; Dawson, 1963). Dental plates are supported by anteroventrally situated basal plate cartilages (Fig. 1B) and, during feeding, are pulled in and out of the mouth *via* retractor and protractor muscle groups (Fig. 2). When feeding, hagfish occasionally tie their bodies into knots to forcefully remove chunks of flesh from large carcasses (Martini, 1998). A single posteriorly curved tooth situated in the

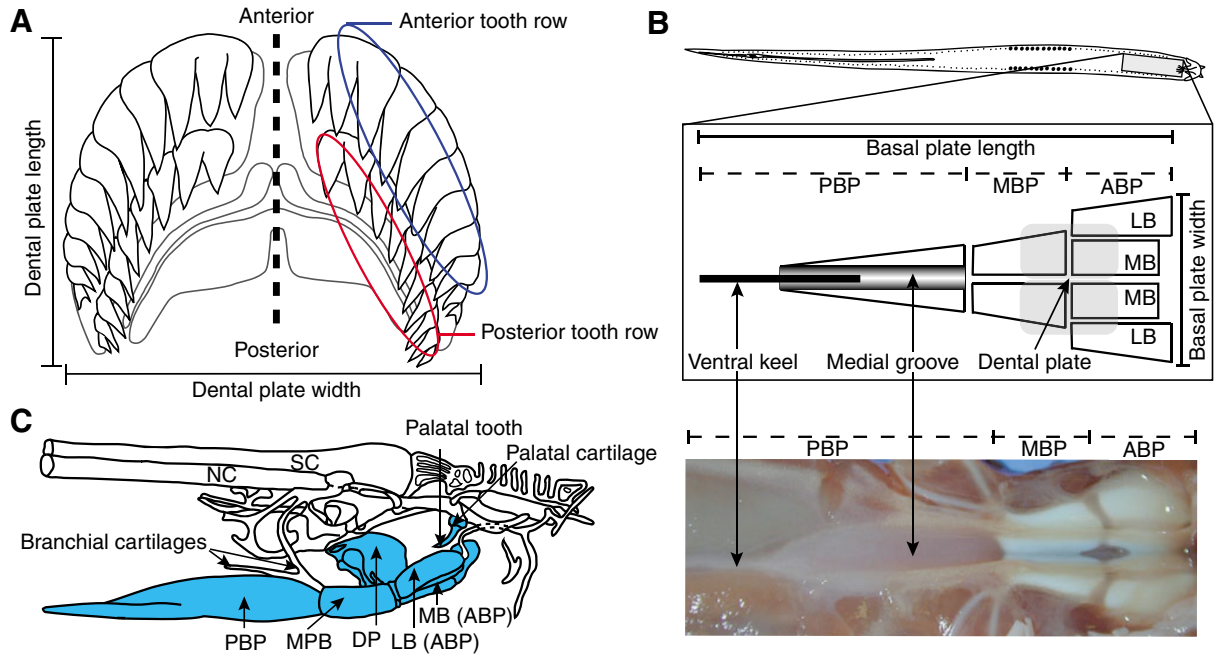

Fig. 1. Skeletal and dental components of the hagfish feeding apparatus. (A) Dorsal view of an unfolded dental plate (oral mucosa removed) from *Eptatretus stoutii*, including methods for measuring dental plate width and dental plate length. Thick broken vertical line represents the axis about which bilateral folding occurs. Anterior and posterior tooth rows are indicated by blue and red outlined ovals, respectively. 2–3 medial teeth in each row are fused and fusion patterns of these medial teeth vary with species. For example, a *M. glutinosa* specimen would have two fused medial teeth in the anterior row (Ferholm, 1998). (B) Ventral view of an *E. stoutii* with the gray box representing the position of the basal plate. The inset shows a schematic of the basal plate in ventral view with the resting position of the dental plate and methods for measuring basal plate length and width. Below is a photograph of a basal plate in dorsal view. ABP, anterior basal plate; MBP, middle basal plate; PBP, posterior basal plate; LB, lateral bar; MB, medial bar. (C) Lateral view of the cranial skeleton of *M. glutinosa*, including the notochord (NC) and spinal cord (SC). Material highlighted in blue represents the cartilages and teeth of the feeding apparatus. DP, dental plate. Image has been modified from (Cole, 1905).

palate augments knot-tying behaviors by allowing a hagfish to anchor itself to the prey (Fig. 1C) (Cole, 1905; Dawson, 1963).

Though we cannot directly apply what we learn from the extant jawless fishes to their armored, and in some cases exceedingly large, ancestors, studying jawless feeding systems is a useful window into the functional advantages provided by jaws. In this study, we aim to (1) compare the morphology of the feeding apparatus of two hagfish species, *Eptatretus stoutii* and *Myxine glutinosa*, (2) compare the feeding kinematics in *E. stoutii* and *M. glutinosa*, (3) calculate forces generated by the musculature during feeding, (4) propose a physical model of the hagfish feeding mechanism, and (5) compare hagfish feeding performance to that of gnathostomes to evaluate the functional constraints of jawlessness. We employed dissection, morphometrics and video techniques to address the following hypotheses: (1) there is little or no interspecific variation in feeding morphology and mechanics between *E. stoutii* and *M. glutinosa*, as dietary diversity is minimal in hagfishes and (2) the absence of jaws and a rigid skeleton limits force generation in hagfish feeding muscles and dental plate protraction–retraction speed.

Materials and methods

Animal care

Care and handling of all living specimens were performed ethically, though as invertebrate chordates hagfish are not required to be covered by an animal care protocol. Live Pacific hagfish, *Eptatretus stoutii* (Lockington) were obtained from Scripps Institute of Oceanography (La Jolla, CA, USA) and live Atlantic hagfish, *Myxine glutinosa* Linnaeus, were obtained from Mount Desert Island Biological Laboratories (Salisbury Cove, ME, USA). Both species were housed together in aquaria with recirculating artificial saltwater maintained at approximately 10°C and 34 p.p.t. (Gustafson, 1935). Most animals were housed in an aquarium (58.42 cm×33.02 cm×33.02 cm) with shades and a cover to block ambient light and to prevent escape. Experimental specimens were filmed feeding in a smaller aquarium (50.80 cm×25.4 cm×31.75 cm) under moderate lighting from two 15 W fluorescent lamps. Individual animals in the smaller aquarium were corralled in a filming area (17.78 cm×30.48 cm×33.20 cm) bordered with perforated white plastic sheets. The smaller aquarium remained unlit when individuals were not being filmed. For maintenance, animals were fed small pieces of squid once every 2 weeks.

Morphology

We dissected and measured dental plate dimensions (length and width), basal plate dimensions (length and width), and hagfish feeding apparatus (HFA) length in eight *E. stoutii* (total length, *TL*=21.0–42.0 cm) and eight *M. glutinosa* (*TL*=33.5–40.5 cm) (Figs 1, 2). Measurements were expressed as percentage of specimen *TL*. In five *E. stoutii*

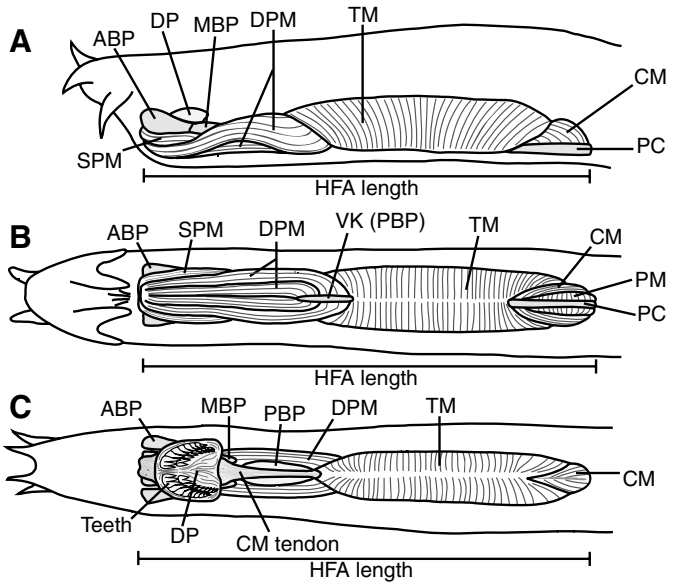

Fig. 2. Morphology of the hagfish feeding apparatus (HFA) in the retracted position and methods for measuring HFA length in (A) lateral view, (B) ventral view and (C) dorsal view. ABP, anterior basal plate; CM, clavatus muscle; DPM, deep protractor muscle; DP, dental plate; MBP, middle basal plate; PBP, posterior basal plate; PC, perpendicularis cartilage; PM, perpendicularis muscle; VK, ventral keel; SPM, superficial protractor muscle; TM, tubulatus muscle. Dental plate cartilages (not shown in C) are covered by oral mucosa.

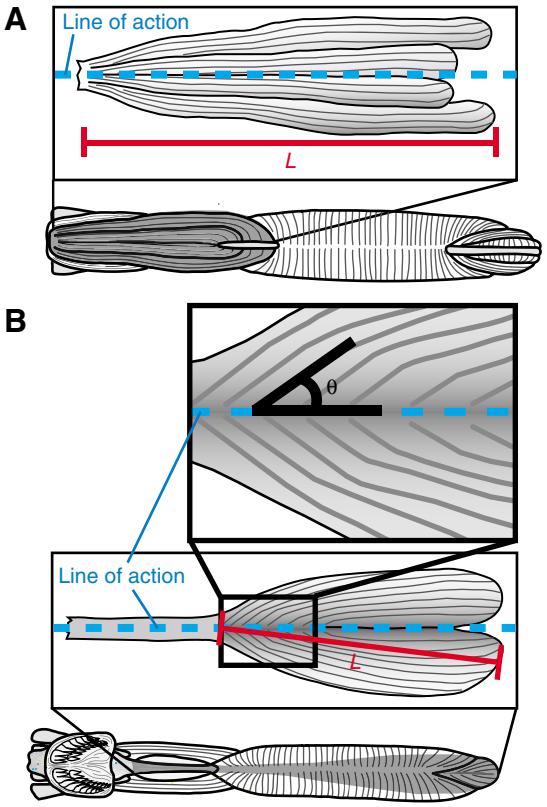

Fig. 3. Schematics showing measurement techniques for determining physiological cross-sectional area and theoretical maximum force production in the clavatus muscle (CM) and deep protractor muscle (DPM). (A) Fiber angle measurements did not apply to the DPM, as DPM fibers coursed parallel with the line of action (broken blue line). (B) Lower inset shows that the two heads of the CM separate once it is removed from the feeding apparatus. Upper inset demonstrates how pennation angles were measured. Fiber angles θ are identical near the muscle's midline (line of action) and begin to vary slightly as they course posteriorly, therefore fiber angles were measured near the muscle's midline. Muscle length *L* was used as a proxy for determining fiber length because mean fiber lengths in the DPM and CM were approximately equal to respective muscle lengths. Darkened areas on the feeding apparatuses indicate positions of the CM and DPM in dorsal and ventral views, respectively. Individual CM and DPM (from insets) are not drawn to scale.

(*TL*=27.0–37.5 cm) and five *M. glutinosa* (*TL*=35.0–40.5 cm), we calculated physiological cross-sectional area (PCSA) and theoretical maximum force production (P_o) of the clavatus muscles (CM) and deep protractor muscles (DPM) (Fig. 3). These two antagonistic muscles directly control dental plate retraction and protraction. Clavatus and deep protractor muscles were weighed to the nearest 0.01 mg and stored in isotonic artificial seawater (~34 p.p.t.). Muscles were stained with iodine to distinguish muscle fibers, and muscle tissue from one specimen was digested with nitric acid to separate muscle fibers (Tamaki et al., 1989). Fiber length was equal to muscle length (L_M) in both the clavatus and deep protractor muscles, therefore we used muscle length in calculating PCSA (Fig. 3). Muscle length was measured with digital calipers to the nearest 0.01 mm. We used published methods (Powell et al., 1984) in calculating PCSA, in which the product of muscle mass (M) and cosine of muscle pennation angle (θ) was divided by the product of muscle density (ρ) and muscle length (L_M), which we substituted for fiber length:

$$\mathrm{PCSA_{CM}} = (M\cos\theta) / (\rho L_M) . \quad (1)$$

Because deep protractor muscle fibers course parallel to the line of action (Fig. 3A), we set θ equal to 0. To determine θ for the clavatus, we stained the muscles and digitally photographed them with a camera mounted on a microscope (Zeiss Stemi 2000-C, Jena, Germany). Fiber pennation angles (θ) were measured with Image J software (NIH) (Fig. 3B). Because hagfish feeding muscles consist of fast-glycolytic fibers (Baldwin et al., 1991), we assumed that the specific tension of hagfish white muscle (K) would approximately equal the specific tension of elasmobranch white muscle (289 kPa) (Lou et al., 1999). We calculated P_o by multiplying the PCSA of each muscle by K (Powell et al., 1984):

$$P_o = \mathrm{PCSA} \times K . \quad (2)$$

Feeding kinematics

Hagfish were selected based on their willingness to feed. Once shifted to the filming tank, an animal was offered rectangular portions (1.0 cm×2.0 cm×0.25 cm) of squid. Each squid was loosely secured to a plastic tie and then positioned directly in front of, and sometimes touching, the animal's mouth. Feeding behaviors were recorded with a JVC digital camcorder at 30 frames s^{-1}, an appropriate frame rate for the

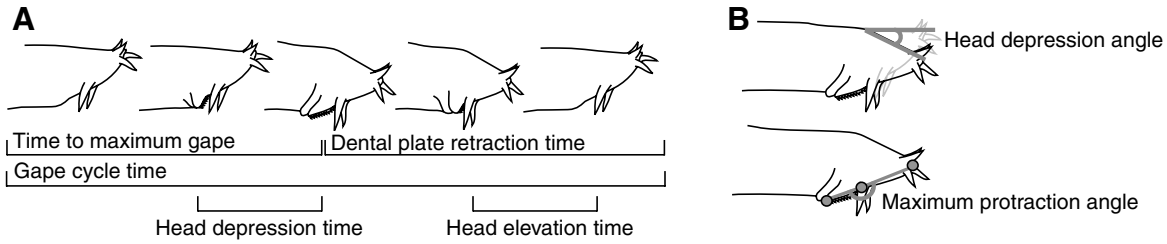

Fig. 4. Measurement schemes for feeding kinematic timing and angular variables in hagfish. (A) Gape cycle time is the elapsed time for maximal dental plate protraction and retraction. Time to maximum gape is the elapsed time to attain maximal dental plate protraction from a retracted position. Dental plate retraction time is the elapsed time to retract the dental plate from a maximally protracted position. Head depression time is the elapsed time from the onset to the completion of head depression. Head elevation time is the elapsed time from the onset to completion of head elevation from a maximally depressed state. (B) Kinematic angular variables defined. Lateral view of a hagfish with a maximally depressed head and a maximally protracted dental plate. Head depression angle (top) is the angle between the anterior tip of the snout before the onset of head depression (see light gray image), the pivoting point of the head, and the anterior tip of snout once the head is maximally depressed. Maximum protraction angle is the angle between the anterior tip of the snout, mouth opening and anterior tip of the maximally protracted dental plate.

feeding performance of these animals (see Movie 1 in supplementary material).

We collected dental plate kinematic data from five specimens of *M. glutinosa* (*TL*=32.0–42.0 cm) and three specimens of *E. stoutii* (*TL*=28.0–38.0 cm). We analyzed 9–31 feeding bouts from each *M. glutinosa* and 5–18 from each *E. stoutii*, with 5–10 min intervals between feeding bouts. Dental plate kinematic variables included gape cycle time, time to maximum gape, dental plate retraction time, and maximum protraction angle. Gape cycle time (GCT) was defined as the time required for a hagfish to fully protract and retract its dental plate (Fig. 4A). Time to maximum gape (TMG) was the elapsed time for maximal dental plate protraction to be attained from a retracted position (Fig. 4A). Dental plate retraction time (DPRT) was the elapsed time for dental plate retraction from a maximally protracted position (Fig. 4A). From both hagfish species, we also compared mean GCT and mean TMG from capture and transport phases (Table 1). We defined maximum protraction angle (MPA) as the angle between the anterior tip of the maximally protracted dental plate, the mouth opening, and the anterior tip of the snout (Fig. 4B).

Kinematic data determined from cranial movements other than dental plate movements were obtained from 11 feeding bouts in two specimens of *E. stoutii* (*TL*=29.0 cm and 38.0 cm) and 25 feeding bouts in four specimens of *M. glutinosa* (*TL*=32.0–37.5 cm). Cranial kinematic variables included head depression angle (Fig. 4B), head depression time (Fig. 4A) and head elevation time (Fig. 4A). Head depression angle (HDA) was the angle between the anterior tip of the snout just before the onset of head depression, the pivoting point of the head, and the anterior tip of the snout once the head was maximally depressed (Fig. 4B). Head depression time (HDT) was the elapsed time from the onset to the completion of head depression (Fig. 4A). Head elevation time (HET) was the elapsed time from the onset to completion of head elevation from a maximally depressed state (Fig. 4A). Cranial kinematic variables were only recorded from food transport phases. MPA and HDA were measured with Image J software (NIH). We only used lateral views of hagfish feeding events for determining MPA and HDA. Time variables (GCT, TMG, DPRT, HDT and HET) were only recorded from video clips that clearly showed dental plate and cranial movements.

Because of a limited sample size and size-range of *E. stoutii* and *M. glutinosa*, we could not accurately scale hagfish GCT with length. However for comparative purposes, we plotted the relationship between body length and GCT from both hagfish species in this study and from most of the gnathostome species listed in the Appendix. From these data, we graphed the relationship between body length and GCT in aquatic and terrestrial feeding craniates.

Statistical analyses

We used a one-way analysis of variance (ANOVA) in SPSS 12.0 to compare the means of dental plate dimensions, basal plate dimensions, HFA length, GCT, TMG, DPRT, MPA,

Table 1. *Gape cycle time (GCT) and time to maximum gape (TMG) from capture and transport feeding events in Eptatretus stoutii and Myxine glutinosa*

Species	Kinematic variable	Capture (ms)	*N* (capture)	Transport (ms)	*N* (transport)	*P*-value
E. stoutii	GCT	931±214	22	1166±265	28	0.001
	TMG	328±116	18	395±107	11	0.137
M. glutinosa	GCT	932±460	41	852±348	40	0.380
	TMG	341±163	41	342±149	40	0.995

Values are means ± s.d.; *N* is the count for capture and transport behaviors.
P-values were determined using one-way ANOVA.

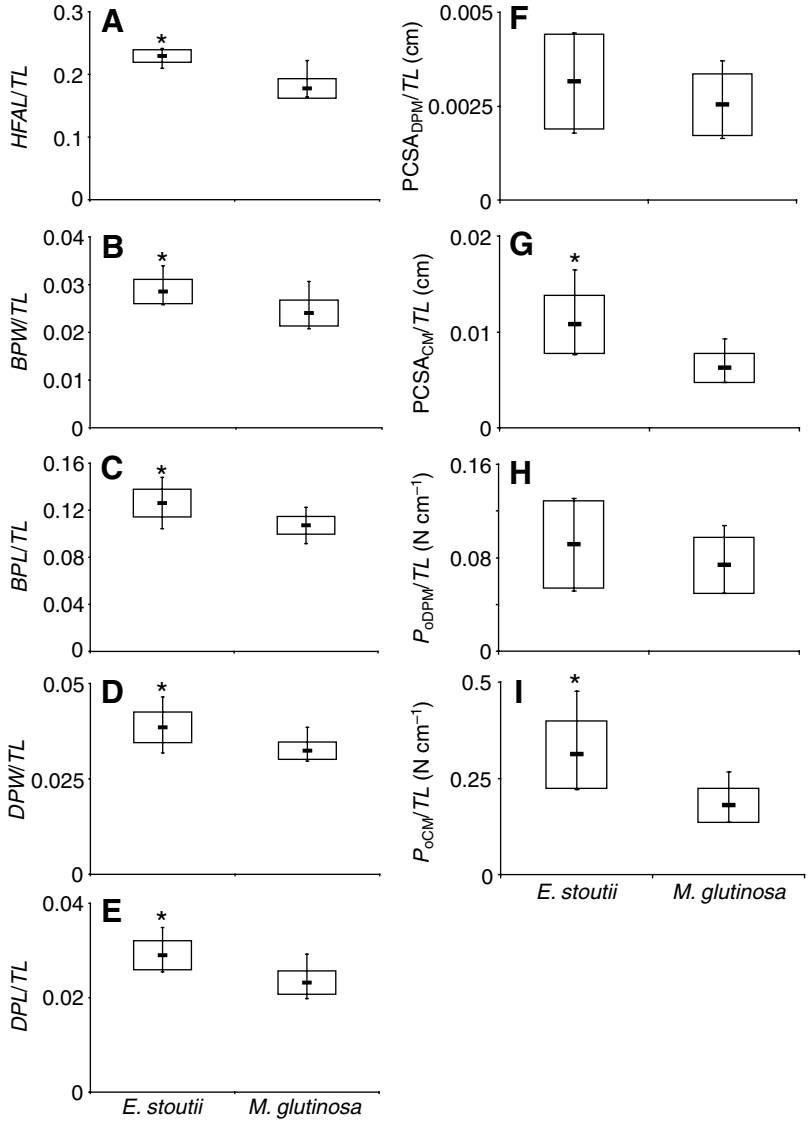

Fig. 5. Box and whisker plots of length-scaled measurements of skeletal dimensions, physiological cross-sectional areas (PCSA), and theoretical maximum muscle force production (P_o) in *Eptatretus stoutii* and *Myxine glutinosa*. Measurements include length-scaled (A) hagfish feeding apparatus length (*HFAL/TL*), (B) basal plate width (*BPW/TL*), (C) basal plate length (*BPL/TL*), (D) dental plate width (*DPW/TL*), (E) dental plate length (*DPL/TL*), (F) deep protractor muscle PCSA (PCSA$_{DPM}$/*TL*), (G) clavatus muscle PCSA (PCSA$_{CM}$/*TL*), (H) deep protractor muscle P_o (P_{oDPM}/*TL*) and (I) clavatus muscle P_o (P_{oCM}/*TL*) in *E. stoutii* and *M. glutinosa.* Each graph includes the 95% confidence interval (box), maximum and minimum values (upper and lower bars, respectively), and a mean value (thick horizontal bar). *Significant difference (P<0.05).

HDA, HDT and HET in *M. glutinosa* and *E. stoutii*. Each species represented an independent group and our test variables included anatomical measurements and kinematic variables. A one-way ANOVA was also used for comparing mean GCT and TMG from food capture and transport phases, in which the feeding phases (food capture or transport) were test variables and kinematic variables were independent groups. The significance level of P=0.05 was used in all analyses.

Least-squares (LS) regressions of GCT and body lengths were plotted in JMPIN (SAS Institute, Cary, NC, USA). Independent (body length) and dependent (GCT) axes were log-transformed in each regression. LS regressions were appropriate for this analysis, as the probability of measurement error is greater in the dependent data (GCT) than in the independent data (body length) (Sokal and Rohlf, 1995). Plots included fitted mean lines (slope of zero) and fitted log-transformed lines with 95% confidence limits. We tested each LS regression for statistical significance (P=0.05) by comparing the slopes of the fitted log-transformed line and fitted mean line using ANOVA.

Results

Morphology and muscle force calculations

Morphology of the hagfish feeding apparatus is illustrated in Figs 1 and 2. For additional reference, excellent descriptions of the morphology of the HFA can be reviewed in the literature (Cole, 1905; Cole, 1907; Dawson, 1963).

When normalized to total length (*TL*), mean HFA length, basal plate dimensions (length and width) and dental plate dimensions (length and width) were significantly greater in *Eptatretus stoutii* (Fig. 5). Normalized feeding apparatus length in *E. stoutii* was 22% longer than in *M. glutinosa*, basal plates were 15% longer and 16% wider, and dental plates were 20% longer and 16% wider.

Neither absolute nor *TL*-scaled deep protractor muscle PCSA and P_o were significantly different in *E. stoutii* and *M. glutinosa*. Deep protractor muscles theoretically exert 2.76–2.99 N on the dental plate during feeding. When scaled to length, mean force production of *E. stoutii* clavatus muscle was significantly larger (10.23 N) than that of *M. glutinosa* (6.73 N) (Fig. 5G,I).

Feeding behavior

Feeding in both *E. stoutii* and *M. glutinosa* can be divided into four general stages: identification, positioning, food ingestion and intraoral transport. Smell and touch appear to be the means by which hagfish identify food. Identification involves independent movement of the tentacles as they contact the food. Simultaneously with or immediately following identification, the mouth is positioned onto or next to the food. Once mouth positioning is established, the food capture (ingestion) stage begins; the dental plates are repeatedly protracted and retracted until the food is engulfed. During protraction, dental plates laterally unfold as they are pulled out of the mouth. Protraction is coupled with simultaneous unveiling of the oral mucosa from the dorsal (toothed) surface of dental plates, which exposes teeth. The toothed surface of the dental plate often slides against the food during protraction. During retraction, the dental plates are pulled back into the mouth. Food becomes hooked on the teeth once retraction begins and becomes even more secure as the dental plates begin to fold medially. Upon entering the mouth, oral mucosa begins to envelope the dental plate, which

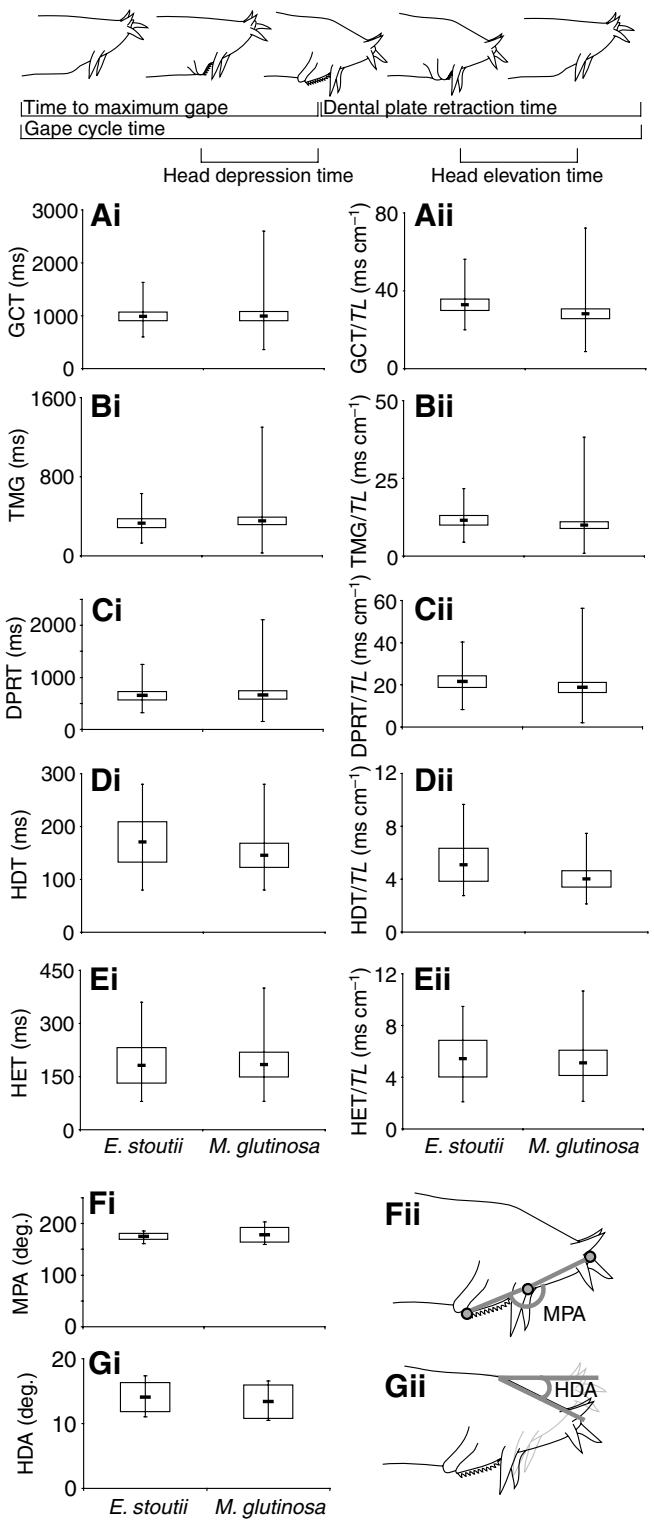

Fig. 6. Box and whisker plots of kinematic variables from *Eptatretus stoutii* and *Myxine glutinosa*, illustrated in the cartoon above. (Ai) Gape cycle time (GCT); (Bi) time to maximum gape (TMG); (Ci) dental plate retraction time (DPRT); (Di) head depression time (HDT); (Ei) head elevation time (HET); (Fi,Fii) maximum protraction angle (MPA); and (Gi,Gii) head depression angle (HDA). Each graph includes the 95% confidence interval (box), maximum and minimum values (upper and lower bars, respectively), and a mean value (thick bar). (Aii–Eii) Measurements relative to *TL*.

unhooks the food from the teeth and pushes the food into the esophagus. Intra-oral transport, which begins once food is ingested, involves repeated dental plate protraction and retraction events coupled with repeated head depression and head elevation.

Animals that responded well to filming tank settings typically remained motionless at the bottom of the tank within 30 min of introduction. *M. glutinosa* specimens would lie sprawled and *E. stoutii* specimens would lie coiled. We did not observe any hagfish actively pursuing food. Food was usually positioned just in front of, and sometimes touching the animal to elicit a feeding bout. Approximately 2 out of 10 attempts to feed animals in the filming tank were successful. On average, both hagfish species required 3 dental plate protraction–retraction events to ingest a squid rectangle. Because squid rectangles were loosely secured to their plastic ties, knot-tying behaviors were not observed in any feeding event. Hagfish would engage in knot-tying if food was firmly tied; however, these data were excluded from this study.

Feeding kinematics

Mean GCT, TMG, and DPRT, graphed in Fig. 6 and listed in Table 2, are pooled from both food capture and transport events. Although GCT, TMG, and DPRT varied considerably in both hagfish species, with more variation in *M. glutinosa*, mean values did not differ significantly (Table 2, Fig. 6A–C). GCT averaged about 1 s, one third of which was protraction and two thirds of which were retraction. Mean MPA in *E. stoutii* and *M. glutinosa* were 175° and 178°, respectively, and did not differ significantly (Table 2, Fig. 6F). Mean GCT and mean TMG from capture and transport events were similar in *M. glutinosa* (Table 1). Mean capture and transport TMG were similar in *E. stoutii*; however, mean GCT in *E. stoutii* were significantly longer in food transport events than in food capture events (Table 1).

Cranial movements were similar in *E. stoutii* and *M. glutinosa* during food transport events. We observed no significant differences in head depression times, head elevation times or head depression angles (Table 2, Fig. 6D,E,G). The onset of head depression occurred between the onset of dental plate protraction and the time of maximum gape (Fig. 7). The head would usually remain depressed for 477 ms prior to the onset of head elevation. Head depression time overlap with dental plate retraction time was only apparent in *E. stoutii*; however, head elevation in both species occurred in the final moments of dental plate retraction and was completed by the end of the gape cycle (Fig. 7).

The long GCT in *E. stoutii* and *M. glutinosa* are noticeable outliers of the LS regression of GCT on body lengths for aquatic feeding craniates. The hagfish data lie outside of the 95% confidence limits and are an order of magnitude above the regression line at their respective body length (Fig. 8A). The slopes of the graphs for both aquatic and terrestrial species are significantly different from zero, indicating a significant relationship between body length and GCT (R^2=0.4197; P<0.0001 and R^2=0.3727; P<0.005, respectively) (Fig. 8). GCT increases hypoallometrically in aquatic and terrestrial feeding craniates (b=0.5499 and b=0.4792, respectively).

Table 2. *Kinematic variables from feeding events in Eptatretus stoutii and Myxine glutinosa*

Variable	*E. stoutii*	(*N*)	*M. glutinosa*	(*N*)	Feeding stage	*P*-value
Gape cycle time (ms)	988±215	(29)	993±432	(97)	C and T	0.946
Time to maximum gape (ms)	331±122	(31)	354±188	(98)	C and T	0.519
Dental plate retraction time (ms)	649±210	(29)	662±386	(87)	C and T	0.867
Head depression time (ms)	171±56.8	(11)	146±55.2	(25)	T	0.218
Head elevation time (ms)	182±74.5	(11)	184±84.9	(25)	T	0.942
Maximum protraction angle (degrees)	175±6.25	(7)	178±15.5	(7)	T	0.608
Head depression angle (degrees)	14.1±2.15	(6)	13.2±2.06	(5)	T	0.598

Values from each species are means ± s.d. C=capture, T=transport. *P*-values were determined using one-way ANOVA.

Discussion

Shared functionality of gnathostomes and hagfish

In some respects, the capabilities of the jawless hagfish feeding apparatus are comparable to those of vertebrate jaws. For example, gape size, a combination of gape angle and jaw length, is an important parameter in determining the feeding niche of gnathostomes because it limits the size of prey that can be consumed whole (Hambright, 1991; Luczkovich et al., 1995; Nilsson and Bronmark, 2000). Despite lacking jaws, hagfish can evert their dental plates to an angle of approximately 180°. Among jawed vertebrates, this extreme is achieved during feeding only by snakes (Cundall and Greene, 2000) and algal scrapers such as Loricariid and Mochikid catfishes (Geerinckx et al., 2007), anuran tadpoles (Wassersug and Yamashita, 2001) and the prowfish (*Zaprora silenus*) (Carollo and Rankin, 1998; Clemens and Wilby, 1961). Large gape angles in male *Hippopotamus* (110°) and male *Babirussa* (~180°) are produced for threat displays and not during feeding (Herring, 1972; Herring and Herring, 1974). Because the protraction angle attained in hagfish is so wide, food size is limited only by the perimeter of the soft tissue around the mouth. Though it might appear that a 180° gape is unimportant to a scavenging carnivore, wide protraction angles enable hagfish to remove relatively large pieces of flesh. Returning the dental plate from a long, 180° excursion prior to ingestion imposes strain on prey tissue, which may facilitate dismembering. Removing large portions of food

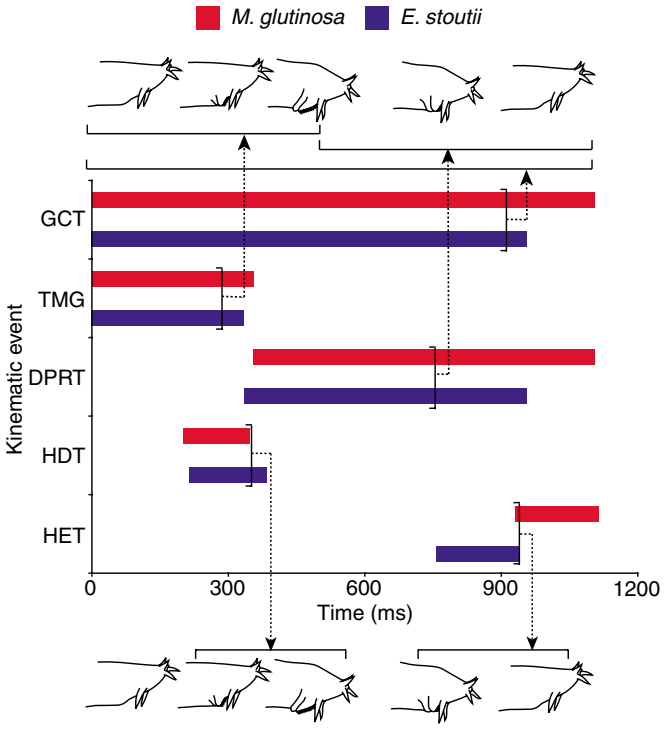

Fig. 7. Cranial kinematic profiles from *Myxine glutinosa* (red) and *Eptatretus stoutii* (blue). Block diagram of relative timing of mean dental plate and cranial kinematic events from two *E. stoutii* (11 food transport events) and four *M. glutinosa* (25 food transport events). GCT, gape cycle time; TMG; time to maximum gape; DPRT, dental plate retraction time; HDT, head depression time; HET, head elevation time.

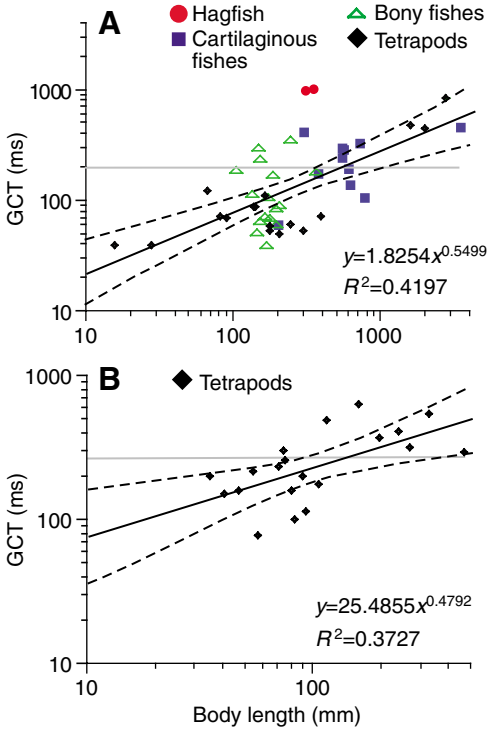

Fig. 8. Gape cycle times (GCT) (in ms) plotted against body lengths (mm) of various craniates. In these plots, body length is represented by total length, standard length, snout–vent length, carapace length and disc width. Horizontal gray lines indicate residual means, broken lines are 95% confidence intervals of the best-fit, least-squares regression (black line). (A) Log-transformed plot of GCT in aquatic feeding craniates. (B) Log-transformed plot of terrestrial feeding tetrapod GCT.

requires fewer feeding bouts, with the potential advantage of less competition with conspecifics and a shorter window of vulnerability in and on a carcass.

Another surprising area where hagfish function as well as gnathostomes is in generating force to accomplish the prey capture cycle. Lacking jaws and a rigid skeleton does not limit the forces that can be generated in hagfish feeding musculature. In lateral view, the HFA can be modeled as a fixed pulley system, in which the input force or speed is equivalent to output force or speed (Fig. 9A). Assuming the effects of friction, inertia and angular changes of the dental plate during protraction and retraction are negligible, the input forces from the feeding muscles are reasonable approximations of the forces exerted by the dental plate. However, in jaws, input forces from muscles are not directly translated to the bite forces (Fig. 9B). We calculated that the mean forces generated by the clavatus and deep protractor muscles of both hagfish species are equal to or exceed the bite forces in four wrasse species (Clifton and Motta, 1998), six turtle species (Herrel et al., 2002), and several (27) finch species (van der Meij and Bout, 2004). Bite force in jaws and the rasping force in dental plates are important parameters for feeding performance because the amount of force can determine the hardness of food that can be processed and the amount of food that can be held in the mouth. Bite force measurements serve as an index for diet and demonstrate how cranial morphology influences the ecology of a species (Hernandez and Motta, 1997; Herrel et al., 2001; Huber et al., 2005; Wainwright, 1987). Considering the absence of jaws and forelimbs in hagfish, the forces exerted on dental plates are necessary for grasping and processing chunks of flesh.

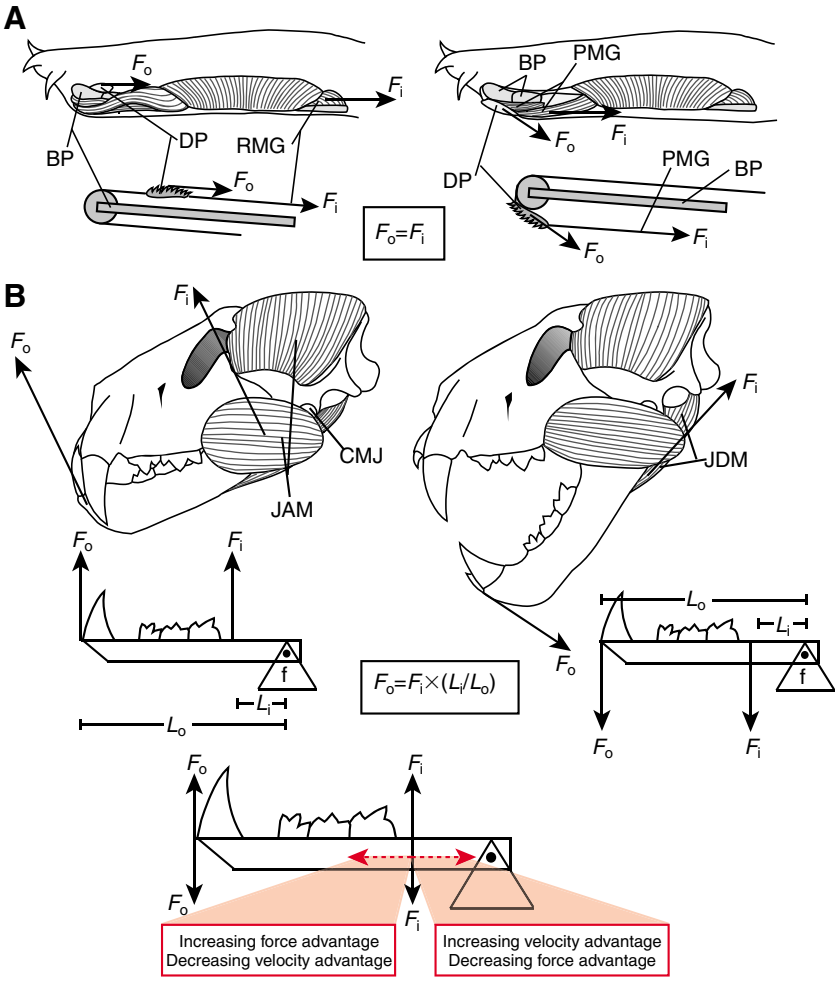

Fig. 9. Physical models of dental plate and jaw kinematics in hagfish and gnathostomes, respectively. (A) Pulley system model for dental plate retraction (left) and protraction (right). (B) Third-order lever system model for jaw adduction (left) and jaw abduction (right) in a large cat (*Panthera*). Dotted red arrows demonstrate how a jaw can be geared for closing velocity or mechanical advantage by changing relative input lever arm lengths (output lever arm remains unchanged in this example). BP, basal plate; CMJ, craniomandibular joint; DP, dental plate; f, fulcrum; F_i, input force; F_o, output force; JAM, jaw adductor muscle; JDM, jaw depressor muscle; L_i, length of input lever arm; L_o, length of output lever arm; PMG, protractor muscle group; RMG, retractor muscle group.

Estimated force production in the deep protractor muscles (DPM) and clavatus muscles (CM) and their roles in feeding demonstrate a clear trade-off in force and speed. DPM are longitudinal muscles designed for relatively rapid, yet less forceful protraction of the dental plate while the clavatus muscle is a bipennate muscle that retracts the dental plate more slowly but with greater force. Clavatus muscle force, which is almost an order of magnitude greater than that of the deep protractor muscle, is comparable to some gnathostome jaw closing muscles. The force generated by the clavatus muscle is transmitted to the dental plates *via* the clavatus tendon, which has been shown to be as strong (47.8±3.5 MPa) and stiff (290±29 MPa) as some gnathostome tendons (Summers and Koob, 2002). Considering the high forces generated in retracting musculature, it is not surprising that the clavatus tendon has a similar response to load as in gnathostome tendons.

Because hagfish feeding forces and gapes are comparable to, or in some cases exceed, the forces and gapes in gnathostomes, we can assume that vertebrate jaws are not prerequisites for producing considerable muscle forces and wide gapes. Challenges other than muscle force and wide gape may have been associated with the selective pressures placed on the gnathostome common ancestor. Extant phylogenetic bracketing (EPB) can infer obscure traits, such as feeding mechanics in extinct agnathans and the common ancestor to gnathostomes. Causal biological relationships between preservable traits (e.g. hard tissue) and unpreservable traits (e.g. soft tissue and behavior) determine the degree of likelihood (level of inference) of obscure traits occurring in extinct taxa (Witmer, 1995). EPB is a well-supported method for reconstructing unclear scenarios in a phylogenetic context (Barrett and Rayfield, 2006; Carrano, 2000; Erickson et al., 2002; Jasinoski et al., 2006; Perry and

Sander, 2004). Our results demonstrate a probable causal relationship between preservable cranial endoskeletons and unpreservable traits such as feeding muscle force and wide gapes. Because this relationship is maintained in hagfishes and gnathostomes, we can assume with a minimal level of speculation [level 1 inference (*sensu* Witmer, 1995)] that muscle force production and wide gapes are characteristic of all agnathan taxa and therefore are not functional innovations of craniate jaws.

Jaws: improving prey capture

In general all gnathostome species bite faster than hagfish (Appendix, Fig. 8). Rapid jaw movements are important in the capture of elusive prey. Furthermore, short GCT and TMG are required to generate the low buccal pressures of suction feeding, a common means of food capture in the aquatic medium (Grubich and Wainwright, 1997; Lauder, 1980; Liem, 1990; Svanback et al., 2002). Dental plate GCT and TMG are long in hagfish, making it difficult to feed on active prey. Although gentle ciliary-generated suction needed for filter feeding is the primitive mode in chordates (occurring in both urochordates and cephalochordates), it is not the immediate precursor to the strong suction seen in most aquatic vertebrates. Instead, a grasping-tearing mode induced by repeated movements of muscularly suspended cartilaginous dental plates appears to be the intermediate.

The significant correlation between GCT and body size across various species of aquatic and terrestrial feeding craniates shows both that hagfish are slow for their size and that the scaling relationship for terrestrial and aquatic feeders is similar (Fig. 8). The GCT of both aquatic and terrestrial feeders scales approximately with $L^{0.5}$. That is, feeding in water appears to require similar speed per length as feeding on land. This could indicate that the scaling of GCT with body size is independent of prey capture mode. For example, suction feeding, the dominant prey capture mode in the aquatic medium, does not impose shorter GCT per unit body length in aquatic feeders than in terrestrial feeders.

The functional flexibility of the gnathostome feeding apparatus, at the individual level, and in an evolutionary context, is driven by the system of levers and kinetic chains that determines kinematic parameters (Westneat, 1990; Westneat, 2004). In general, jaws are third order levers or 4-bar linkages geared to increase closing velocity. In hagfish, the muscular attachments on the dental plate, and movement of the dental plate about the basal plate, resemble a fixed pulley, which neither offers speed nor force amplification as in levers or linkages (Fig. 9). The key innovation of jaws may be that they allow a lever system or linkage system to increase kinematic transmission efficiency (KT) of the jaw muscles at the expense of high force transmission (Fig. 9B).

Interspecific variation in hagfish feeding

The differences in feeding apparatus morphology between these two hagfish species beg further studies of morphology and diet. Although the diet of *M. glutinosa* is more known than that of *E. stoutii*, marine invertebrates appear to be the primary diet in both species (Martini, 1998). The more robust apparatus of *E. stoutii* relative to *M. glutinosa* is supported by larger dental plates that have more area for dentition. Presumably the larger number of teeth in *E. stoutii* allows them to grasp prey more firmly. Greater inertial resistance of the dental plates might explain the greater force we calculated in *E. stoutii* clavatus muscles. However, these morphological disparities do not have significant effects on the kinematics of feeding, except that *E. stoutii* has a longer gape cycle time during the transport phase and head depression generally overlaps the onset of dental plate retraction. We suppose that the morphological differences between *E. stoutii* and *M. glutinosa* are barely manifested in feeding kinematics because (1) morphological disparity is not always translated to feeding behavior and mechanics (Hulsey and Wainwright, 2002) or (2) the particular kinematics we examined are unaffected by the morphological parameters we measured.

Conclusions

In summary, bite speed appears to be a major functional innovation allowed by jaws. Even the most basal gnathostomes, the arthrodire placoderms, managed to overcome the constraint of heavy dermal cranial armor with 4-bar linkages of considerable KT (Anderson and Westneat, 2006). The configuration of the jawless hagfish feeding apparatus as a fixed pulley provides both an advantage, minimal reduction in force transmitted from the feeding muscles to dental plates, and a disadvantage, impaired rapid dental plate movements. Lever and linkage systems in vertebrate jaws permit functional flexibility, enabling gnathostomes to occupy a diversity of dietary niches. Nevertheless, hagfish protract their dental plates to extremely wide angles rarely attained by jawed vertebrates and posses feeding muscles that can generate forces comparable to that in some gnathostomes. Our data, coupled with EPB principles, suggest that generating considerable muscular forces and attaining wide gape angles were present in the common ancestor to the craniates, not the common ancestor to gnathostomes. Long gape cycle time, wide protraction angle, and considerable muscle force in hagfish are suitable for a diet consisting of dead or dying prey. The feeding mechanism in hagfish, which also occurs in lampreys and possibly some extinct agnathan lineages (Janvier, 1993; Yalden, 1985), appears to be an intermediate form between the cephalochordates and gnathostomes. Morphological variation exists in the feeding apparatuses of *E. stoutii* and *M. glutinosa*, nevertheless the feeding mechanism is conserved in both species.

List of abbreviations

ρ	muscle density
θ	muscle pennation angle
ANOVA	analysis of variance
CM	clavatus muscle
DPM	deep protractor muscle
DPRT	dental plate retraction time
EPB	extant phylogenetic bracketing
GCT	gape cycle time
HDA	head depression angle
HDT	head depression time
HET	head elevation time
HFA	hagfish feeding apparatus

K	specific tension	MPA	maximum protraction angle
KT	kinematic transmission efficiency	PCSA	physiological cross-sectional area
L_M	muscle length	P_o	maximum force production
LS	least-squares	TL	total length
M	muscle mass	TMG	time to maximum gape

Appendix

Species	GCT (ms)	TMG (ms)	GA (degrees)	Length (cm)	Source
Hagfishes					
Eptatretus stoutii	986	331	175	31.7	Present study
Myxine glutinosa	993	354	178	36.3	Present study
Cartilaginous fishes					
Carcharhinus perezi	383	120	N/A	N/A	(Motta and Wilga, 2001)
Ginglymostoma cirratum	100	32	N/A	78	(Motta et al., 2002)
Carcharodon carcharias	443	140	N/A	350	(Tricas and McCosker, 1984)
Cephaloscyllium ventriosum	N/A	327*	84.6*	30	(Ferry-Graham, 1997)
Heterodontus francisci	131*	54.2*	N/A	62.5	(Edmonds et al., 2001)
Negaprion brevirostris	309	81	N/A	72.3†	(Motta et al., 1997)
Rhinobatos lentiginosus	274‡	133‡	N/A	57	(Wilga and Motta, 1998b)
Squalus acanthias	280	100	N/A	55.5	(Wilga and Motta, 1998a)
Sphyrna tiburo	186	103	33	60.7	(Wilga and Motta, 2000)
Triakis semifasciata	165	97.5	82.6	38.1	(Ferry-Graham, 1998)
Narcine brasiliensis	58	N/A	N/A	20.0	(Dean and Motta, 2004)
Rhinoptera bonasus	233	N/A	77	55.0 (*DW*)	(Sasko et al., 2006)
Bony fishes					
Antennarius hispidus	N/A	6.3	N/A	9.8	(Grobecker and Pietsch, 1979)
Antennarius striatus	N/A	6.2	N/A	8.2	(Grobecker and Pietsch, 1979)
Antennarius maculatus	N/A	6.7	N/A	6.3	(Grobecker and Pietsch, 1979)
Micropterus salmoides	89	N/A	N/A	20.6	(Richard and Wainwright, 1995)
Pleuronichthys verticalis	39	20.0	33.8	17	(Gibb, 1995)
Xystreurys liolepis	69.5	31.4	33.5	16.5	(Gibb, 1996)
Pleuronectes platessa	103.5	N/A	N/A	17.4† (*SL*)	(Bels and Davenport, 1996)
Limanda limanda	293.6	N/A	N/A	15† (*SL*)	(Bels and Davenport, 1996)
Scaphirhynchus albus	180	76	N/A	37.3	(Carroll and Wainwright, 2003)
Choerodon anchorago	168.2	101.5	23.2	19	(Ferry-Graham et al., 2002)
Coris gaimard	83.2	41.1	23.3	19.8	(Ferry-Graham et al., 2002)
Hologymnosus doliatus	60.3	28.4	16.7	19.8	(Ferry-Graham et al., 2002)
Novaculichthys taeniourus	64.4	32.2	36.4	15.4	(Ferry-Graham et al., 2002)
Oxycheilinus digrammus	68.3	35.7	23.8	18	(Ferry-Graham et al., 2002)
Lepomis macrochirus	51	29.4	30.8	14.6	(Gillis and Lauder, 1995)
Pomacanthus semicirculatus	345	300	N/A	24.7	(Konow and Bellwood, 2005)
Hippocampus erectus	N/A	4.9	N/A	6.05	(Bergert and Wainwright, 1997)
Syngnathus floridae	N/A	6.8	N/A	16.2	(Bergert and Wainwright, 1997)
Salvelinus fontinalis	N/A	47.2	31.1	15.9	(Sanford, 2001)
Osteoglossum bicirrhosum	N/A	69.9	29.3	14.5	(Sanford and Lauder, 1990)
Pantodon buchholzi	N/A	28.8	18.7	6.1	(Sanford and Lauder, 1990)
Notopterus chitala	N/A	64.4	10	26.8	(Sanford and Lauder, 1990)
Clariallabes longicauda	196	N/A	58	3.8 (*CRL*)	(Van Wassenbergh et al., 2004)
Clarias gariepinus	225	75	33.1	4.9 (*CRL*)	(Van Wassenbergh et al., 2004)
Acanthurus nigrofuscus	184	N/A	112.8	10.7† (*SL*)	(Purcell and Bellwood, 1993)
Ctenochaetus striatus	233	N/A	177.6	15.2 (*SL*)	(Purcell and Bellwood, 1993)
Epibulus insidiator	111.3	N/A	N/A	13.8	(Westneat and Wainwright, 1989)
Tetrapods					
Chelodina longicollis	110	N/A	N/A	16.5 (*CL*)	(Van Damme and Aerts, 1997)
Chelydra serpentina	88.3	46.3	31.9	14.2 (*CL*)	(Lauder and Prendergast, 1992)
Tupinambis teguixin	542	429	19	32.8	(Elias et al., 2000)
Varanus exanthematicus	412	302.5	16.5	24.4	(Elias et al., 2000)
Caiman crocodilus	300	N/A	46	47.5	(Cleuren and Devree, 1992)
Ambystoma mexicanum	69.7	33.8	N/A	9.1	(Shaffer and Lauder, 1985)
Ambystoma dumerilii	88	46.7	N/A	14	(Shaffer and Lauder, 1985)
Ambystoma ordinarium	73	38	N/A	8.3	(Shaffer and Lauder, 1985)

Appendix continued on next page.

Appendix *(continued)*

Species	GCT (ms)	TMG (ms)	GA (degrees)	Length (cm)	Source
Tetrapods					
Phelsuma madagascariensis	180	140	39.3	10.8	(Delheusy and Bels, 1999)
Oplurus cuvieri	500	450	33.1	11.7	(Delheusy and Bels, 1992)
Cryptobranchus allegheniensis	53.3	30	N/A	30.0	(Reilly and Lauder, 1992)
Dicamptodon tenebrosus	54.4	29	N/A	18.0	(Reilly and Lauder, 1992)
Ambystoma mexicanum	59	26.4	N/A	18.0	(Reilly and Lauder, 1992)
Amphiuma means	72	31.5	N/A	40.0	(Reilly and Lauder, 1992)
Necturus maculosus	51	23	N/A	21.0	(Reilly and Lauder, 1992)
Siren intermedia	61	29	N/A	25.0	(Reilly and Lauder, 1992)
Agama stellio	374	45	42	20	(Herrel et al., 1995)
Uromastix acanthinurus	640.5	427.5	29.8	16.2	(Herrel and De Vree, 1999)
Moloch horridus	116	65	47.2	9.4	(Meyers and Herrel, 2005)
Pogona vitticeps	307	269	29.5	7.4	(Meyers and Herrel, 2005)
Phyrnosoma platyrhinos	263	235	50.9	7.6	(Meyers and Herrel, 2005)
Uma notata	200	179	24.1	9.1	(Meyers and Herrel, 2005)
Agkistrodon piscivorus	N/A	65	69.9	55.8	(Vincent et al., 2005)
Terrapene carolina	N/A	420	N/A	11.8	(Summers et al., 1998)
Tursiops truncatus	863	564	25	278.5	(Bloodworth and Marshall, 2005)
Kogia breviceps	447	282[§]	40[§]	203	(Bloodworth and Marshall, 2005)
Kogia sima	482	282[§]	40[§]	160	(Bloodworth and Marshall, 2005)
Pachymedusa dacnicolor	120*	49*	119*	N/A	(Gray and Nishikawa, 1995)
Rana caesbeiana (tadpole)	125*	47.5*	150*	6.8	(Wassersug and Yamashita, 2001)
Salamandra salamandra (stage 1)	39.8	18	35	1.6 (*SVL*)	(Reilly, 1995)
Salamandra salamandra (stage 2)	40.3	17.1	32.3	2.8 (*SVL*)	(Reilly, 1995)
Hyla cinerea	152	57	79	4.1[†] (*SVL*)	(Deban and Nishikawa, 1992)
Tylototriton verrucosus	159.3	100.4	44.8	8.2[†] (*SVL*)	(Miller and Larsen, 1990)
Pleurodeles waltl	220	147.3	53.3	5.5[†] (*SVL*)	(Miller and Larsen, 1990)
Cynops pyrrhogaster	161.7	110.4	71.9	4.8[†] (*SVL*)	(Miller and Larsen, 1990)
Paramesotriton hongkongensis	237.5	190.7	51.7	7.1 (*SVL*)	(Miller and Larsen, 1990)
Pachytriton brevipes	79.4	25	87	5.8 (*SVL*)	(Miller and Larsen, 1990)
Salamandra salamandra	100.2	61.1	58.9	8.4[†] (*SVL*)	(Miller and Larsen, 1990)
Salamandra terdigitata	203.6	120	51.5	3.6[†] (*SVL*)	(Miller and Larsen, 1990)
Tiliqua scincoides	317.3*	199.6*	20.5*	27.1 (*SVL*)	(Smith et al., 1999)

*Mean from different food types (size, prey species, etc.) and different feeding behaviors (drop, miss, etc.).
[†]Mean length calculated of maximum and minimum lengths.
[‡]Ingestion/capture phase only.
[§]Pooled from both species of *Kogia*.
DW, disc width; *CRL*, cranial length; *SL*, standard length; *CL*, carapace length; *SVL*, snout–vent length.

Eddie Kisfaludy and Tom Koob generously provided Pacific and Atlantic specimens, respectively. Sabreena Kasbati, Ahmed Ibrahim, and Peggy Kozick assisted with aquarium maintenance. Drafts of this manuscript were improved by critical, intellectual input from two anonymous reviewers, Kate Loudon, Doug Fudge, the Comparative Physiology Group and Biomechanics Labs at UCI. We thank the National Science Foundation (IOB-0616322 awarded to A.P.S.) and the American Physiological Society for a Porter Fellowship awarded to A.J.C.

References

Anderson, P. S. L. and Westneat, M. W. (2006). Feeding mechanics and bite force modeling of the skull of *Dunkleosteus terrelli*, an ancient apex predator. *Biol. Lett.* **3**, 76-79.
Baldwin, J., Davison, W. and Forster, M. E. (1991). Anaerobic glycolysis in the dental plate retractor muscles of the New Zealand hagfish *Eptatretus cirrhatus* during feeding. *J. Exp. Biol.* **260**, 295-301.
Bardack, D. (1991). First fossil hagfish (Myxinoidea) – a record from the Pennsylvanian of Illinois. *Science* **254**, 701-703.
Barrett, P. M. and Rayfield, E. J. (2006). Ecological and evolutionary implications of dinosaur feeding behaviour. *Trends Ecol. Evol.* **21**, 217-224.
Bels, V. L. and Davenport, J. (1996). A comparison of food capture and ingestion in juveniles of two flatfish species, *Pleuronectes platessa* and *Limanda limanda* (Teleostei: Pleuronectiformes). *J. Fish Biol.* **49**, 390-401.
Bergert, B. A. and Wainwright, P. C. (1997). Morphology and kinematics of prey capture in the syngnathid fishes *Hippocampus erectus* and *Syngnathus floridae*. *Mar. Biol.* **127**, 563-570.
Bloodworth, B. and Marshall, C. D. (2005). Feeding kinematics of *Kogia* and *Tursiops* (Odontoceti: Cetacea): characterization of suction and ram feeding. *J. Exp. Biol.* **208**, 3721-3730.
Carollo, M. and Rankin, P. (1998). The care and display of the prowfish, *Zaprora silenus*. *Drum Croaker* **29**, 3-6.
Carrano, M. T. (2000). Homoplasy and the evolution of dinosaur locomotion. *Paleobiology* **26**, 489-512.
Carroll, A. M. and Wainwright, P. C. (2003). Functional morphology of prey capture in the sturgeon, *Scaphirhynchus albus*. *J. Morphol.* **256**, 270-284.
Carroll, R. L. (1988). *Vertebrate Paleontology and Evolution*. New York: W. H. Freeman.
Clemens, W. A. and Wilby, G. V. (1961). Fishes of the Pacific coast of Canada. *Fish. Res. Board Can. Bull.* **68**, 443.
Cleuren, J. and Devree, F. (1992). Kinematics of the jaw and hyolingual apparatus during feeding in *Caiman crocodilus*. *J. Morphol.* **212**, 141-154.
Clifton, K. B. and Motta, P. J. (1998). Feeding morphology, diet, and

ecomorphological relationships among five Caribbean labrids (Teleostei, Labridae). *Copeia* **1998**, 953-966.
Cole, F. J. (1905). A monograph of the general morphology of the myxinoid fishes, based on a study of Myxine. Part I. The anatomy of the skeleton. *Trans. R. Soc. Edinb.* **41**, 749-788.
Cole, F. J. (1907). A monograph of the general morphology of the myxinoid fishes, based on a study of Myxine. Part 2. The anatomy of the muscles. *Trans. R. Soc. Edinb.* **45**, 683-757.
Cundall, D. and Greene, H. (2000). Feeding in snakes. In *Feeding: Form, Function, and Evolution in Tetrapod Vertebrates* (ed. K. Schwenk), pp. 293-333. San Diego: Academic Press.
Dawson, J. A. (1963). The oral cavity, the 'jaws' and the horny teeth of *Myxine glutinosa*. In *The Biology of Myxine* (ed. A. B. Fange and R. Fange), pp. 231-255. Oslo: Universitetsforlaget.
Dean, M. N. and Motta, P. J. (2004). Feeding behavior and kinematics of the lesser electric ray, *Narcine brasiliensis* (Elasmobranchii: Batoidea). *Zoology* **107**, 171-189.
Deban, S. M. and Nishikawa, K. C. (1992). The kinematics of prey capture and the mechanism of tongue protraction in the green tree frog *Hyla cinerea*. *J. Exp. Biol.* **170**, 235-256.
Delheusy, V. and Bels, V. L. (1992). Kinematics of feeding-behavior in *Oplurus cuvieri* (Reptilia, Iguanidae). *J. Exp. Biol.* **170**, 155-186.
Delheusy, V. and Bels, V. L. (1999). Feeding kinematics of *Phelsuma madagascariensis* (Reptilia: Gekkonidae): testing differences between Iguania and Scleroglossa. *J. Exp. Biol.* **202**, 3715-3730.
Edmonds, M. A., Motta, P. J. and Hueter, R. E. (2001). Food capture kinematics of the suction feeding horn shark, *Heterodontus francisci*. *Environ. Biol. Fish.* **62**, 415-427.
Elias, J. A., McBrayer, L. D. and Reilly, S. M. (2000). Prey transport kinematics in *Tupinambis teguixin* and *Varanus exanthematicus*: Conservation of feeding behavior in 'chemosensory-tongued' lizards. *J. Exp. Biol.* **203**, 791-801.
Erickson, G. M., Catanese, J. and Keaveny, T. M. (2002). Evolution of the biomechanical material properties of the femur. *Anat. Rec.* **268**, 115-124.
Fernholm, B. (1998). Hagfish systematics. In *The Biology of Hagfishes* (ed. J. M. Jørgensen, R. E. Weber and H. Malte), pp. 33-44. London: Chapman & Hall.
Ferry-Graham, L. A. (1997). Feeding kinematics of juvenile swellsharks, *Cephaloscyllium ventriosum*. *J. Exp. Biol.* **200**, 1255-1269.
Ferry-Graham, L. A. (1998). Effects of prey size and mobility on prey-capture kinematics in leopard sharks *Triakis semifasciata*. *J. Exp. Biol.* **201**, 2433-2444.
Ferry-Graham, L. A., Wainwright, P. C., Westneat, M. W. and Bellwood, D. R. (2002). Mechanisms of benthic prey capture in wrasses (Labridae). *Mar. Biol.* **141**, 819-830.
Geerinckx, T., Brunain, M., Herrel, A., Aerts, P. and Adriaens, D. (2007). A head with a suckermouth: a functional-morphological study of the head of the suckermouth armoured catfish *Ancistrus* cf. *triradiatus* (Loridariidae, Siluriformes). *Belg. J. Zool.* **137**, 47-66.
Gibb, A. C. (1995). Kinematics of prey capture in a flatfish, *Pleuronichthys verticalis*. *J. Exp. Biol.* **198**, 1173-1183.
Gibb, A. C. (1996). Of prey capture in *Xystreurys liolepis*: do all flatfish feed asymmetrically? *J. Exp. Biol.* **199**, 2269-2283.
Gillis, G. B. and Lauder, G. V. (1995). Kinematics of feeding in bluegill sunfish – is there a general distinction between aquatic capture and transport behaviors. *J. Exp. Biol.* **198**, 709-720.
Gray, L. A. and Nishikawa, K. C. (1995). Feeding kinematics of phyllomedusine tree frogs. *J. Exp. Biol.* **198**, 457-463.
Grobecker, D. B. and Pietsch, T. W. (1979). High-speed cinematographic evidence for ultrafast feeding in antennariid angler-fishes. *Science* **205**, 1161-1162.
Grubich, J. R. and Wainwright, P. C. (1997). Motor basis of suction feeding performance in largemouth bass, *Micropterus salmoides*. *J. Exp. Zool.* **277**, 1-13.
Gustafson, G. (1935). On the biology of *Myxine glutinosa*. *Ark. Zool.* **28A**, 1-8.
Hambright, K. D. (1991). Experimental analysis of prey selection by largemouth bass: role of predator mouth width and prey body depth. *Trans. Am. Fish. Soc.* **120**, 500-508.
Hernandez, L. P. and Motta, P. J. (1997). Trophic consequences of differential performance: ontogeny of oral jaw-crushing performance in the sheepshead, *Archosargus probatocephalus* (Teleostei, Sparidae). *J. Zool.* **243**, 737-756.
Herrel, A. and De Vree, F. (1999). Kinematics of intraoral transport and swallowing in the herbivorous lizard *Uromastix acanthinurus*. *J. Exp. Biol.* **202**, 1127-1137.
Herrel, A., Cleuren, J. and Devree, F. (1995). Prey capture in the lizard *Agama stellio*. *J. Morphol.* **224**, 313-329.
Herrel, A., De Grauw, E. and Lemos-Espinal, J. A. (2001). Head shape and bite performance in xenosaurid lizards. *J. Exp. Zool.* **290**, 101-107.
Herrel, A., O'Reilly, J. C. and Richmond, A. M. (2002). Evolution of bite performance in turtles. *J. Evol. Biol.* **15**, 1083-1094.
Herring, S. W. (1972). Role of canine morphology in evolutionary divergence of pigs and peccaries. *J. Mammal.* **53**, 500-512.
Herring, S. W. and Herring, S. E. (1974). Superficial masseter and gape in mammals. *Am. Nat.* **108**, 561-576.
Huber, D. R., Eason, T. G., Hueter, R. E. and Motta, P. J. (2005). Analysis of the bite force and mechanical design of the feeding mechanism of the durophagous horn shark *Heterodontus francisci*. *J. Exp. Biol.* **208**, 3553-3571.
Hulsey, C. D. and Wainwright, P. C. (2002). Projecting mechanics into morphospace: disparity in the feeding system of labrid fishes. *Proc. R. Soc. Lond. B Biol. Sci.* **269**, 317-326.
Janvier, P. (1993). Patterns of diversity in the skull of jawless fishes. In *The Skull: Patterns of Structural and Systematic Diversity* (ed. J. Hanken and B. K. Hall), pp. 131-188. Chicago, London: The University of Chicago Press.
Jasinoski, S. C., Russell, A. P. and Currie, P. J. (2006). An integrative phylogenetic and extrapolatory approach to the reconstruction of dromaeosaur (Theropoda: Eumaniraptora) shoulder musculature. *Zool. J. Linn. Soc.* **146**, 301-344.
Konow, N. and Bellwood, D. R. (2005). Prey-capture in *Pomacanthus semicirculatus* (Teleostei, Pomacanthidae): functional implications of intramandibular joints in marine angelfishes. *J. Exp. Biol.* **208**, 1421-1433.
Lauder, G. V. (1980). Evolution of the feeding mechanism in primitive actinopterygian fishes – a functional anatomical analysis of *Polypterus*, *Lepisosteus*, and *Amia*. *J. Morphol.* **163**, 283-317.
Lauder, G. V. and Prendergast, T. (1992). Kinematics of aquatic prey capture in the snapping turtle *Chelydra serpentina*. *J. Exp. Biol.* **164**, 55-78.
Liem, K. F. (1990). Aquatic versus terrestrial feeding modes – possible impacts on the trophic ecology of vertebrates. *Am. Zool.* **30**, 209-221.
Liem, K. F., Bemis, W. E., Walker, J. W. F. and Grande, L. (2001). *Functional Anatomy Of The Vertebrates: An Evolutionary Perspective*. Belmont, CA: Brooks/Cole-Thomson Learning.
Lou, F., Curtin, N. A. and Woledge, R. C. (1999). Elastic energy storage and release in white muscle from dogfish *Scyliorhinus canicula*. *J. Exp. Biol.* **202**, 135-142.
Luczkovich, J. J., Motta, P. J., Norton, S. F. and Liem, K. F. (1995). The role of ecomorphological studies in the comparative biology of fishes. *Environ. Biol. Fish.* **44**, 287-304.
Mallatt, J. (1996). Ventilation and the origin of jawed vertebrates: a new mouth. *Zool. J. Linn. Soc.* **117**, 329-404.
Martini, F. (1998). The ecology of hagfishes. In *The Biology of Hagfishes* (ed. J. M. Jørgensen, R. E. Weber and H. Malte), pp. 57-77. London: Chapman & Hall.
Meyers, J. and Herrel, A. (2005). Prey capture kinematics of ant-eating lizards. *J. Exp. Biol.* **208**, 113-127.
Miller, B. T. and Larsen, J. H., Jr (1990). Comparative kinematics of terrestrial prey capture in salamanders and newts (Amphibia: Urodela: Salamandridae). *J. Exp. Biol.* **256**, 135-153.
Motta, P. J. and Wilga, C. D. (2001). Advances in the study of feeding behaviors, mechanisms, and mechanics of sharks. *Environ. Biol. Fish.* **60**, 131-156.
Motta, P. J., Tricas, T. C., Hueter, R. E. and Summers, A. P. (1997). Feeding mechanism and functional morphology of the jaws of the lemon shark *Negaprion brevirostris* (Chondrichthyes, Carcharhinidae). *J. Exp. Biol.* **200**, 2765-2780.
Motta, P. J., Hueter, R. E., Tricas, T. C. and Summers, A. P. (2002). Kinematic analysis of suction feeding in the nurse shark, *Ginglymostoma cirratum* (Orectolobiformes, Ginglymostomatidae). *Copeia* **2002**, 24-38.
Nilsson, P. A. and Bronmark, C. (2000). Prey vulnerability to a gape-size limited predator: behavioural and morphological impacts on northern pike piscivory. *Oikos* **88**, 539-546.
Perry, S. F. and Sander, M. (2004). Reconstructing the evolution of the respiratory apparatus in tetrapods. *Respir. Physiol. Neurobiol.* **144**, 125-139.
Powell, P. L., Roy, R. R., Kanim, P., Bello, M. A. and Edgerton, V. R. (1984). Predictability of skeletal muscle tension from architectural determinations in guinea pig hindlimbs. *J. Appl. Physiol.* **57**, 1715-1721.
Purcell, S. W. and Bellwood, D. R. (1993). A functional-analysis of food procurement in 2 surgeonfish species, *Acanthurus nigrofuscus* and *Ctenochaetus striatus* (Acanthuridae). *Environ. Biol. Fish.* **37**, 139-159.
Purnell, M. A. (2002). Feeding in extinct jawless heterostracan fishes and testing scenarios of early vertebrate evolution. *Proc. R. Soc. Lond. B Biol. Sci.* **269**, 83-88.
Reilly, S. M. (1995). The ontogeny of aquatic feeding behavior in *Salamandra*

salamandra: stereotypy and isometry in feeding kinematics. *J. Exp. Biol.* **198**, 701-708.

Reilly, S. M. and Lauder, G. V. (1992). Morphology, behavior, and evolution – comparative kinematics of aquatic feeding in salamanders. *Brain Behav. Evol.* **40**, 182-196.

Richard, B. A. and Wainwright, P. C. (1995). Scaling the feeding mechanism of largemouth bass (*Micropterus salmoides*): kinematics of prey capture. *J. Exp. Biol.* **198**, 419-433.

Sanford, C. P. J. (2001). Kinematic analysis of a novel feeding mechanism in the brook trout *Salvelinus fontinalis* (Teleostei: Salmonidae): behavioral modulation of a functional novelty. *J. Exp. Biol.* **204**, 3905-3916.

Sanford, C. P. J. and Lauder, G. V. (1990). Kinematics of the tongue – bite apparatus in osteoglossomorph fishes. *J. Exp. Biol.* **154**, 137-162.

Sasko, D. E., Dean, M. N., Motta, P. J. and Hueter, R. E. (2006). Prey capture behavior and kinematics of the Atlantic cownose ray, *Rhinoptera bonasus*. *Zoology* **109**, 171-181.

Shaffer, H. B. and Lauder, G. V. (1985). Patterns of variation in aquatic ambystomatid salamanders – kinematics of the feeding mechanism. *Evolution* **39**, 83-92.

Smith, T. L., Kardong, K. V. and Bels, V. L. (1999). Prey capture behavior in the blue-tongued skink, *Tiliqua scincoides*. *J. Herpetol.* **33**, 362-369.

Sokal, R. R. and Rohlf, F. J. (1995). *Biometry*. New York: W. H. Freeman.

Summers, A. P. and Koob, T. J. (2002). The evolution of tendon – morphology and material properties. *Comp. Biochem. Physiol.* **133A**, 1159-1170.

Summers, A. P., Darouian, K. F., Richmond, A. M. and Brainerd, E. L. (1998). Kinematics of aquatic and terrestrial prey capture in *Terrapene carolina*, with implications for the evolution of feeding in cryptodire turtles. *J. Exp. Zool.* **281**, 280-287.

Svanback, R., Wainwright, P. C. and Ferry-Graham, L. A. (2002). Linking cranial kinematics, buccal pressure, and suction feeding performance in largemouth bass. *Physiol. Biochem. Zool.* **75**, 532-543.

Tamaki, T., Akatsuka, A., Itoh, J. and Nakano, S. (1989). A newly modified isolation method of single muscle fibers: especially useful in histological, histochemical and electron microscopic studies on branched fibers. *Tokai J. Exp. Clin. Med.* **14**, 211-218.

Tricas, T. C. and McCosker, J. E. (1984). Predatory behavior of the white shark (*Carcharodon carcharias*), with notes on its biology. *Proc. Calif. Acad. Sci.* **43**, 221-238.

Van Damme, J. and Aerts, P. (1997). Kinematics and functional morphology of aquatic feeding in Australian snake-necked turtles (Pleurodira; Chelodina). *J. Morphol.* **233**, 113-125.

van der Meij, M. A. A. and Bout, R. G. (2004). Scaling of jaw muscle size and maximal bite force in finches. *J. Exp. Biol.* **207**, 2745-2753.

Van Wassenbergh, S., Herrel, A., Adriaens, D. and Aerts, P. (2004). Effects of jaw adductor hypertrophy on buccal expansions during feeding of air breathing catfishes (Teleostei: Clariidae). *Zoomorphology* **123**, 81-93.

Vincent, S. E., Herrel, A. and Irschick, D. J. (2005). Comparisons of aquatic versus terrestrial predatory strikes in the pitviper, *Agkistrodon piscivorus*. *J. Exp. Zool. Part A* **303**, 476-488.

Wainwright, P. C. (1987). Biomechanical limits to ecological performance – mollusk-crushing by the caribbean hogfish, *Lachnolaimus maximus* (Labridae). *J. Zool.* **213**, 283-297.

Wassersug, R. J. and Yamashita, M. (2001). Plasticity and constraints on feeding kinematics in anuran larvae. *Comp. Biochem. Physiol.* **131A**, 183-195.

Westneat, M. W. (1990). Feeding mechanics of teleost fishes (Labridae, Perciformes) – a test of 4-Bar Linkage models. *J. Morphol.* **205**, 269-295.

Westneat, M. W. (2004). Evolution of levers and linkages in the feeding mechanisms of fishes. *Integr. Comp. Biol.* **44**, 378-389.

Westneat, M. W. and Wainwright, P. C. (1989). Feeding mechanism of *Epibulus insidiator* (Labridae, Teleostei) – evolution of a novel functional system. *J. Morphol.* **202**, 129-150.

Wilga, C. D. and Motta, P. J. (1998a). Conservation and variation in the feeding mechanism of the spiny dogfish *Squalus acanthias*. *J. Exp. Biol.* **201**, 1345-1358.

Wilga, C. D. and Motta, P. J. (1998b). Feeding mechanism of the Atlantic guitarfish *Rhinobatos lentiginosus*: modulation of kinematic and motor activity. *J. Exp. Biol.* **201**, 3167-3184.

Wilga, C. D. and Motta, P. J. (2000). Durophagy in sharks: feeding mechanics of the hammerhead *Sphyrna tiburo*. *J. Exp. Biol.* **203**, 2781-2796.

Witmer, L. M. (1995). The extant phylogenetic bracket and the importance of reconstructing soft tissues in fossils. In *Functional Morphology in Vertebrate Paleontology* (ed. J. J. Thomason), pp. 19-33. New York: Cambridge University Press.

Yalden, D. W. (1985). Feeding mechanisms as evidence for cyclostome monophyly. *Zool. J. Linn. Soc.* **84**, 291-300.